Path following: from mobile robotics to laser surgery

Jean-Antoine Seon, Brahim Tamadazte, Nicolas Andreff

Abstract— **Laser surgery requires accurate following of a path defined by the surgeon, while the velocity on this path is dependent on the laser-tissue interaction. Therefore, path following and velocity profile control must be decoupled. In this paper, non-holonomic control of the unicycle model is used to implement velocity-independent visual path following for laser microphonosurgery. Experiments at almost 600 Hz show an accuracy (mean) of less than 0.34 pixels ($\approx 15\ \mu$m) with a standard deviation of 0.21 pixels ($\approx 10\mu$m) in path following, and a relative velocity distortion of 7.5×10^{-8} %.**

I. INTRODUCTION

Laser surgery consists of the use of a laser source (instead of a scalpel) to cut tissue in which the laser beam vaporizes soft tissue. A large variety of surgical areas practice laser surgery: ophthalmology, gynaecology, otolaryngology, neurosurgery, and paediatric surgery [1]. This is especially true when it comes to microsurgery which requires an extreme precision [2]. In the past few decades, the microphonosurgery received a growing interest by both surgeons and researchers in the objective to develop more suitable and intuitive laser microsurgery system [3], especially in the laser-assisted procedure field. Vocal folds surgery is one of the most demanding procedures in terms of accuracy, particularly because of the specific tissue to be resected (thin, viscous, fragile, difficult healing, and lesions less than 1 mm) [4].
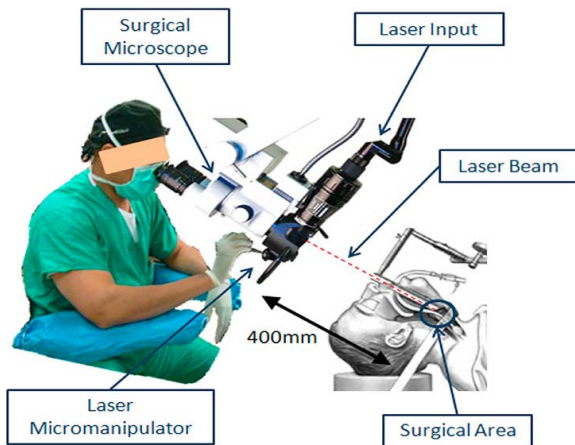

Fig. 1: Schematic view of the laser steering system with two cameras.

The most popular laser-assisted microphonosurgery is undoubtedly the AcuBlade system [5]. The later consists of a laser micromanipulator placed outside the patient which is manually actuated by the surgeon. The use of this system requires extensive expertise due to the position of the laser source (positioned from a distance of 400 mm) (Fig. 1). Consequently, the laser surgery performances are highly dependent on the individual surgeon dexterity and skills [6], [7]. To overcome this drawbacks, the μRALP project develops a more compact (less than 20 mm of diameter) and intuitive flexible endoscopic system [8]. It can be inserted directly into the larynx and equipped with cameras, lighting source, laser source and two degrees of freedom (dof) steered mirror [9] to control the laser spot displacement on the target. This new system allows the monitoring of ablation and resection of the vocal folds tumors in automatic mode. It means that the laser displacement on the vocal folds is steered by controlling the embedded 2 dof mirror using a vision feedback control scheme.
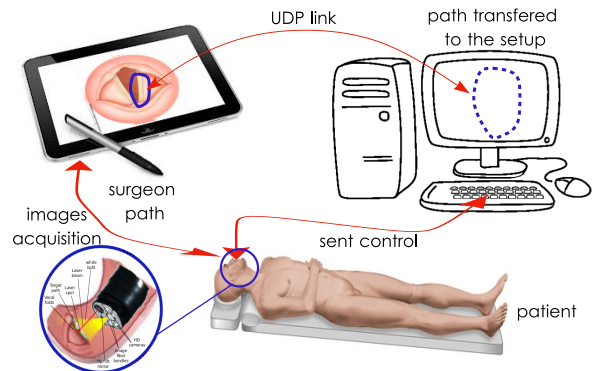

Fig. 2: Schematic view of the laser steering system with two cameras.

In practice, the control consists of two tasks. The first one is to ensure the laser velocity compatibility with laser-tissue interaction, in order to avoid carbonization of the tissue while achieving efficient incision or ablation. The second one is to ensure that the laser follows the desired geometric path drawn by the surgeon on the input device (a tablet in [8]) (Fig. 2). Those two tasks eventually define the trajectory (i.e., geometric path + velocity profile along the path) of the laser. However, it is not advisable to use standard trajectory tracking because the two tasks should be intuitively modifiable by the surgeon. In this paper, we focus on the second task: laser path following using the visual feedback independently from the velocity profile.

The first contribution of the paper is to consider laser

path following as a non-holonomic problem, similar to the unicycle path following (Fig. 3(a)). The second contribution of the paper is to implement path following at high frequency to satisfy the constraints of laser-tissue interaction.

In the remainder of this paper, Section II gives a background on the existing path following methods in mobile robotics. In Section III, the implementation of the path following method is detailed. Section IV presents the experimental validation results.

II. PATH FOLLOWING IN MOBILE ROBOTICS

Path following in the mobile robotics has been widely studied in the literature for many years and there are several applications in the industrial field (e.g., autonomous vehicle control). Path following differs from trajectory following essentially by the fact that the notion of *time* is removed in the first one. Indeed, in trajectory following the robot is controlled to be at a location at a given time which is not the case in path following. However, as shown by Brockett [10], mobile robots are not stable with continuous steady state feedback laws. The first approach is to use discontinuous control laws [12] or piecewise continuous control law [13]. But these methods do not explicitly address the issue of robustness to the occurrence of uncertainties. Thereafter, [14] proposed to use a sliding mode based controller which has shown better behaviors. The second approach is to use continuous non-steady state feedback laws such as Samson in the early 90 [15]. Lyapunov methods are often used to design such type of control law [17], [19]. Indeed, it gives good results in terms of robustness and accuracy. It is also possible to use a chained system to design the controller with exact linearization as shown by Morin and Samson [20], [21]. In these studies, the path following speed profile is not known so, only the path and the distance between the robot and the curve are considered. Therefore, the tangential vectors of the curve are used to set the velocity and the orientation of the robot. In our work, both motion and behavior of a laser spot are considered as analogous to those of a unicycle robot. This means that the displacement of the laser spot on a target is governed by the control of an actuated small mirror on which the laser beam is reflected. The laser spot trajectory will be defined by the surgeon using a tablet or smartphone, on which are projected the vocal folds images in real-time. This trajectory is naturally unknown shape and a non-parameterized curve.

A. Kinematic Equations

Let us consider that the laser spot is represented by a 2D point $\mathbf{p} = (x,y)^\top$ in a fixed (reference) frame $\mathcal{R}_0$ (the image frame). Therefore, the kinematics of the laser are governed in the *Frenet* frame $\mathcal{R}_s$ (Fig. 3(b))frame by:

$$\dot{s} = \frac{v}{1-dC(s)}\cos\theta_e \tag{1}$$

$$\dot{d} = v\sin\theta_e \tag{2}$$

$$\dot{\theta}_e = \omega - \dot{s}C(s) \tag{3}$$

where s and $C(s)$ are respectively the curvilinear abscissa and the curvature, θ_e is the difference between the laser orientation $\underline{\mathbf{v}}$ and the tangential vector of $\mathcal{R}_s$, d is the distance of $\mathbf{p}$ to Γ, v represents the translational velocity amplitude of the laser spot in $\mathcal{R}_0$, and ω its rotational velocity carried by the axis $^0\underline{z}$ (Fig. 3(b)).

B. Control law

To establish the controller, [20] introduces a coordinates/variables transformation in the following manner: $\{s,d,\theta_e,v,\omega\} \iff \{z_1,z_2,z_3,u_1,u_2\}$ defined in $\mathbb{R}^2 \times \left(-\frac{\pi}{2},+\frac{\pi}{2}\right) \times \mathbb{R}^2$. This allows transforming locally (1), (2) and (3) in:

$$\dot{z}_1 = u_1 \tag{4}$$

$$\dot{z}_2 = u_1 z_3 \tag{5}$$

$$\dot{z}_3 = u_2 \tag{6}$$

where u_1 and u_2 are intermediate control inputs.

In our case, the coordinates/variables transformation is defined as:

$$z_1 = s \tag{7}$$

$$z_2 = d \tag{8}$$

$$z_3 = \left(1-dC(s)\right)\tan\theta_e \tag{9}$$

and,

$$u_1 = \dot{s} \tag{10}$$

$$u_2 = \left(-\dot{d}C(s) - d\frac{\partial C(s)}{\partial s}\dot{s}\right)\tan\theta_e \tag{11}$$
$$+ \left(1-dC(s)\right)\left(1+\tan^2\theta_e\right)\dot{\theta}_e$$

Moreover, to ensure that the distance d and the orientation error θ_e are servoed to 0, the stable proportional state feedback solution [20] is:

$$u_2 = -u_1\gamma_1 z_2 - |u_1|\gamma_2 z_3 \tag{12}$$

where, γ_1 and γ_2 are positive gains.

III. IMPLEMENTATION

Considering that the position of the laser spot $\mathbf{p}$ and the curvilinear coordinates s and $C(s)$ are well known at each iterations k of the process, the rotational speed ω can be computed by inverting (11):

$$\omega = \frac{u_2 + \left(\dot{d}C(s) + d\frac{\partial C(s)}{\partial s}\dot{s}\right)\tan\theta_e}{\left(1-dC(s)\right)\left(1+\tan^2\theta_e\right)} + \dot{s}C(s) \tag{13}$$

Then, using (12) and (13) allow defining the expression of the velocity direction at each step k of the path following process:

$$\underline{\mathbf{v}}_{k+1} = \frac{\underline{\mathbf{v}}_k + \omega^0\underline{z} \times \underline{\mathbf{v}}_k}{\|\underline{\mathbf{v}}_k + \omega^0\underline{z} \times \underline{\mathbf{v}}_k\|} \tag{14}$$

where, $\times$ defines the cross-product and $\underline{\mathbf{v}}_k$ represents the current velocity direction of the laser spot.
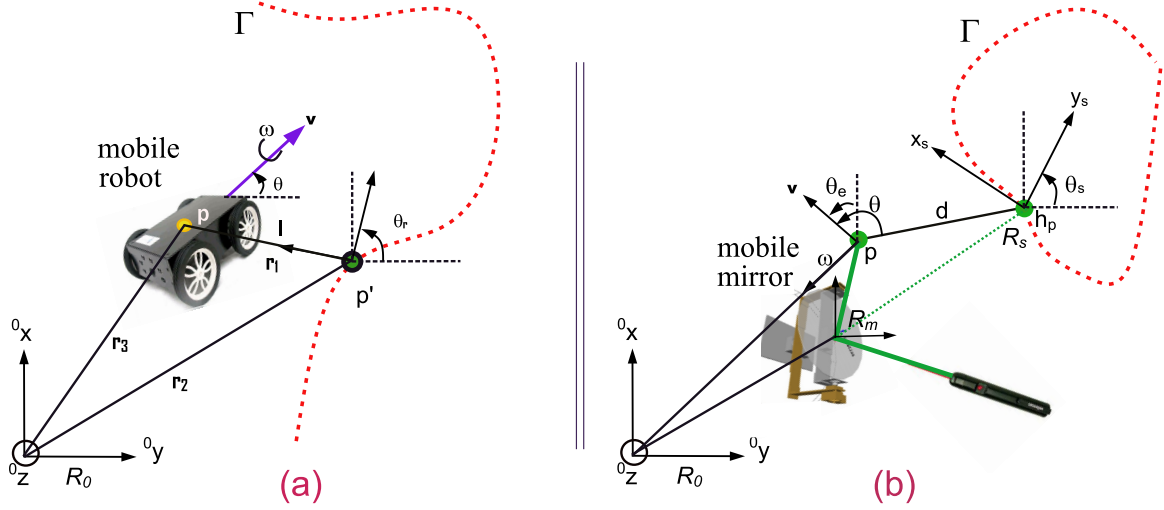
Fig. 3: Mobile robot modeling *versus* laser surgery modeling.

Therefore, it is necessary to convert these velocities to the joint velocities $\dot{\mathbf{q}}_i$ ($i \in [1,2]$) through the inverse differential kinematic matrix $\mathbf{D}^{-1}$ of the mirror mechanism as $\dot{\mathbf{q}}_i = \mathbf{D}^{-1}\begin{pmatrix} \dot{x} \\ \dot{y} \end{pmatrix}$.

IV. VALIDATION

A. Experimental Set-up

The proposed path following technique was tested on a home-made experimental set-up (Fig. 4). It consists of a high speed camera EoSens®CXP (from Mikrotron®) characterized with a frame rate which can reach 10 000 frames per second with a resolution of 800×600 pixels, a laser pointer, a fixed mirror, and an actuated mirror (S-334) from Physical Instruments Inc. The latter contains two single axis units (α and β) working in series with one common pivot point characterized by a bandwidth of 1 kHz, a resolution of 0.2 μrad and a motion range of ± 25 *mrad*. With that motion range and appropriate alignment of the mirror with the image, the inverse kinematics can be approximated by: $\mathbf{D}^{-1} \approx \begin{pmatrix} 1 & 0 \\ 0 & 1 \end{pmatrix}$.

Concerning the time-varying position p of the laser spot in the image, it is tracked using ViSP library [23].

B. Experimental Validation

The proposed method have been implemented on the experimental set-up presented above to verify the relevance of the path following technique. To illustrate the results, we opted for a non-parametric and arbitrary shape curve as shown in Fig. 5. The initial position of the laser spot is placed at a distance $d = 1$ pixel and an orientation $\theta_e = 0$ to the closed point of the curve Γ. The initial parameters (gains) are fixed as $v = 100$, $\gamma_1 = 0.2$, and $\gamma_2 = 0.8$.

Fig. 5 shows an image sequence describing the experimental validation of the proposed path following method. As shown by this figure, the reference path (yellow color) is perfectly followed by the laser spot (red color) even in the
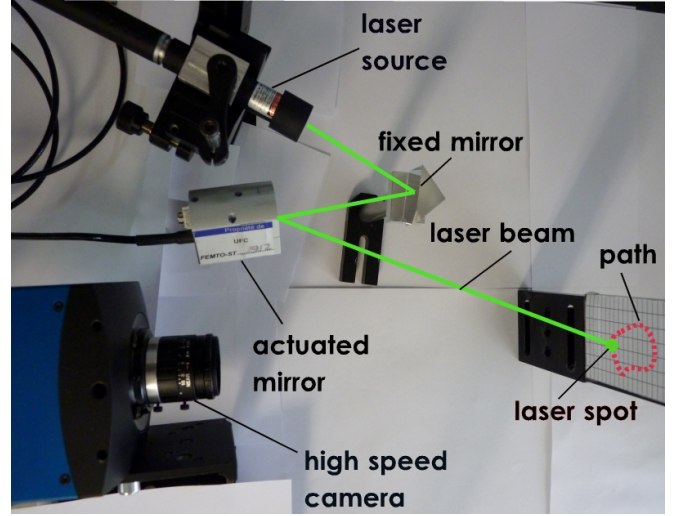

Fig. 4: Photography of the experimental set-up.

case where the curvature is significant. Similarly, Fig. 7(a) illustrates the evolution of the errors (distance d as well as orientation θ_e) *versus* the iterations number k (**each iteration takes 1.702 ms**). For several repetitive tests, the RMS (Root Mean Square) error as well as the standard deviation (STD) are computed (e.g., RMS(d) = 0.34 pixels $\equiv$ 15 μm and STD(d) = 0.21 pixels $\equiv$ 10 μm). Otherwise, the velocity variations are computed and shown in Fig. 6 in which it can be highlighted that the laser spot velocity profile during the entirety process remains almost constant (with a relative velocity distortion of 7.5×10^{-8} %).

Note that in laser microphonosurgery, the laser scanning should works in high frequency i.e., at least of 200 Hz (sampling time) to avoid tissue carbonization during tumors ablation or resection. As shown in Table I, it can be highlighted that our approach takes only 1.702 milliseconds (ms) which is equivalent to a frequency of 587 Hz (sampling time) despite the use of a slow USB communication.
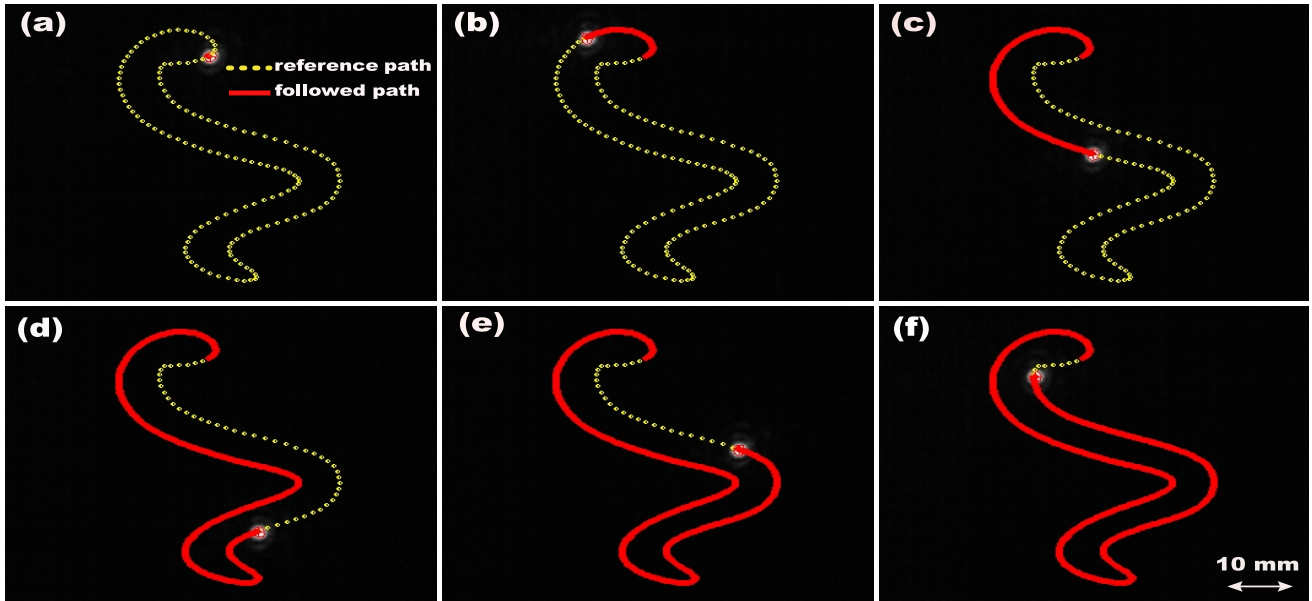
Fig. 5: Image sequence captured during the experimental validation of the path following: (a) to (f) represent the laser spot displacements (in red color) following the reference path (in yellow color).
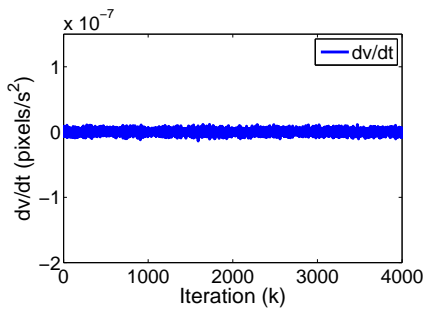

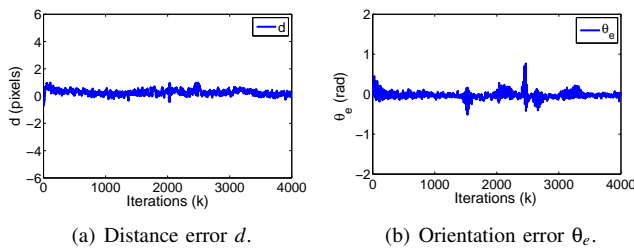Fig. 6: Velocity profile during the path tracking process studied in Fig. 5.

(a) Distance error d.   (b) Orientation error θ_e.

Fig. 7: Experimental results for the validation test shown in Fig. 5.

TABLE I: Time-consuming of the main tasks of the process.

task	time (*ms*)
grabbing image	0.064
laser tracking	0.471
controller	0.002
sending control (USB 2.0)	0.989
others	0.176
entire process	**1.702 (f = 587 Hz)**

We also studied the effect of the velocity **v** on the quality (RMS and standard deviation of the error) for the path following using another shape curve. Thus, for different ranges of velocity **v** from 100 pixels/seconds to 500 pixels/seconds with a step of 100, the accuracy remains almost the same (RMS(d) $\in$ [0.072 to 0.083] pixels, and RMS(θ_e) $\in$ [0.072 to 0.083] rad and standard deviation within similar ranges.

V. CONCLUSION

In this paper, a vision-based control for laser steering using a path following approach was presented. To achieve this, we were inspired explicitly by the methods used in mobile (unicycle kinematic model) in order to develop an efficient controller scheme by taking into account the fact that the path following and the velocity profile must be decoupled. Thus, the proposed path following method was based on the use of the curvilinear representation (i.e., curvilinear abscissa and curvature) which allows a better consideration of the laser steering problem, especially in case of laser surgery. This method was validated experimentally using a real-world validation set-up which was equipped with a high frequency (1 kHz) actuated mirror and high speed camera ($\approx$ 10 000 fps). The developed controller has shown more than satisfactory results in terms of accuracy (about 15 μm), robustness, repeatability and rapidity (about 587 Hz).

The next stages of this work will involve adapting the described materials for real laser surgery applications i.e., on a human cadaver using the entire endoscopy system developed in μRALP project. In addition, the velocity will have to be servoed with regard to the heat profile in the tissue and to the depth variations of the tissues with respect to the image.

REFERENCES

[1] W. Schwesinger and J. Hunter, "Laser in general surgery, in "*Surgical Clinics of North America*, 1992.

[2] V. Moiseev, "Laser technologies in microsurgery of extramedullary tumors, in "*Int. Conf. on Actual Problems of Electronic Instrument Engineering*, 2004, pp. 275–275.

[3] M. Remacle, "Laser-assisted microphonosurgery," in *Surgery of Larynx and Trachea*, M. Remacle and H. E. Eckel, Eds. Springer Berlin Heidelberg, 2010, pp. 51–56.

[4] H. Eckel, S. Berendes, M. Damm, and J. Klusmann, "Suspension laryngoscopy for endotracheal stenting, in "*Laryngoscope*, vol. 113, pp. 11–15, 2003.

[5] L. I. Israel. (2014, Feb.) Digital acublade system. israel@online. [Online]. Available: http://www.surgical.lumenis.com

[6] J. Ortiz, L. Mattos, and D. Caldwell, "Smart devices in robot-assisted laser microsurgery: Towards ubiquitous tele-cooperation," in *IEEE Int. Conf. on Rob. and Biomimetics*, 2012, pp. 1721–1726.

[7] N. Andreff, S. Dembélé, B. Tamadazte, Z. E. Hussnain, "Epipolar geometry for vision-guided laser surgery" in *Int. Conf. on Info. in Cont., Auto. and Robo.*, 2013, pp. 471–476.

[8] L. Mattos, D. Nikhil, G. Barresi, L. Gustani, G. Pirreti, "A novel computerized surgeonmachine interface for robot-assisted laser phonomicrosurgery"; in "Laryngoscope", DOI: 10.1002/lary.24566, 2014.

[9] S. Lescano, D. Zlatanov, M. Rakotondrabe, and N. Andreff, "Kinematic analysis of a meso scale parallel robot for laser phonomicrosurgery," in *IAK 2013 - 2nd Conf. on Interdisciplinary Applications in Kinematics*, A. Kecskemthy, Ed. Springer Berlin, 2013.

[10] R. W. Brockett, "Asymptotic stability and feedback stabilization, "in *Differential Geometric Control Theory*, R. S. M. R. W. Brockett and H. J. Sussmann, Eds. Boston: Birkhauser, 1983, pp. 181–191.

[11] A. Bloch and N. McClamroch, "Control of mechanical systems with classical nonholonomic constraints," in *IEEE Conf. on Decision and Control*, 1989, pp. 201–205.

[12] A. Bloch, M. Reyhanoglu, and N. McClamroch, "Control and stabilization of nonholonomic dynamic systems," in *IEEE Trans. on Automatic Control*, vol. 37, no. 11, pp. 1746–1757, 1992.

[13] J. P. Hespanha, D. Liberzon, and A. Morse, "Logic-based switching control of a nonholonomic system with parametric modeling uncertainty, in"*Systems and Control Letters*, vol. 38(3), pp. 167–177, 1999.

[14] T. Floquet, J.-P. Barbot, and W. Perruquetti, "Higher-order sliding mode stabilization for a class of nonholonomic perturbed systems, in "*Automatica*, vol. 39, no. 6, pp. 1077–1083, 2003.

[15] C. Samson, "Velocity and torque feedback control of a nonholonomic cart," in *Advanced Robot Control*, Lecture Notes in Control and Information Sciences, C. Canudas de Wit, Ed.Springer Berlin Heidelberg, 1991, vol. 162, pp. 125–151.

[16] J.-B. Pomet, "Explicit design of time-varying stabilizing control laws for a class of controllable systems without drift, in "*Systems and Control Letters*, vol. 18, no. 2, pp. 147–158, 1992.

[17] J. Godhavn and O. Egeland, "A lyapunov approach to exponential stabilization of nonholonomic systems in power form," in *IEEE Trans. on Auto. Control*, vol. 42, no. 7, pp. 1028–1032, 1997.

[18] W. E. Dixon, Z. P. Jiang, and D. M. Dawson, "Global exponential setpoint control of wheeled mobile robots: A lyapunov approach," in *Automatica*, vol. 36, pp. 1741–1746, 2000.

[19] M. Aicardi, G. Casalino, A. Bicchi, and A. Balestrino, "Closed loop steering of unicycle like vehicles via lyapunov techniques," in *IEEE Rob. Auto. Mag.*, vol. 2, no. 1, pp. 27–35, 1995.

[20] C. Samson, "Mobile robot control. part 2: Control of chained systems and application to path following and time-varying point stabilization of wheeled vehicles," INRIA, Tech. Rep. 1994.

[21] P. Morin and C. Samson, "Motion control of wheeled mobile robots," in *Springer Handbook of Robotics*, B. Siciliano and O. Khatib, Eds. Springer Berlin Heidelberg, 2008, pp. 799–826.

[22] F. Frenet, "Sur les courbes à double courbure," in *J. des mathématiques pures et appliquées*. Joseph Liouville, 1852, pp. 437–448.

[23] E. Marchand, F. Spindler, and F. Chaumette, "Visp for visual servoing: a generic software platform with a wide class of robot control skills, in"*IEEE Rob. and Auto. Mag.*, vol. 12, no. 4, pp. 40–52, 2005.